

# FIELD EFFECT TRANSISTOR-LIKE CONTROL OF CAPILLARIC FLOW USING OFF-VALVES

Robert Claude Meffan<sup>1,2</sup>, Daniel Mak<sup>1</sup>, Julian Menges<sup>1</sup>, Fabian Dolamore<sup>1</sup>, Conan Fee<sup>1</sup>,  
Renwick C.J. Dobson<sup>1</sup> and Volker Nock<sup>\*1</sup>

<sup>1</sup>Biomolecular Interaction Centre, University of Canterbury, Christchurch, NZ and  
<sup>2</sup>Department of Micro-Engineering, Kyoto University, Kyoto, Japan

## ABSTRACT

An important application area of microfluidics is point-of-care devices. Capillarc circuits are a promising technology to realize such devices. Recently, we introduced a capillary action off-valve which adds pre-programmed autonomous “off”-type valving as a unit operation to capillarc circuits. To date, these devices have only been shown to operate in binary mode. However, due to its conceptual symmetry with electronic junction field effect transistors, it was hypothesized that the off-valve was capable of providing analog resistance control. Using an experimental approach, this work demonstrates for the first time that capillary off-valves can operate in analog resistance mode and that flow control results can be fitted using a modified model of the Shockley transistor equation.

## KEYWORDS

Capillary Off-valves, Capillarc Circuits, Point-of-care Testing, Microfluidics.

## INTRODUCTION

An important emerging area of microfluidics is point-of-care (PoC) devices. The goal of these devices is to facilitate scientific and medical testing outside of the laboratory environment, therefore by necessity excluding all but the most basic scientific tools. While these devices stand to have a widespread and beneficial impact on society [1,2], stringent cost [3], complexity [4], and reliability [5] aspects must be considered [6]. Capillarc circuits are a very promising microfluidic technology for PoC testing that can meet these goals. These devices use the physical structure of a microfluidic channel to control the progress of a liquid meniscus undergoing capillary self-pumping. Available structures include resistors ( $\sim$ ), capillary pumps ( $\square$ ), reservoirs ( $\square$ ) and two-level trigger valves ( $\rightarrow$ ). Addressing the lack of ability to “switch-off” fluid flow in a capillarc circuit systems channels, we have recently introduced capillary action off-valve devices ( $\bullet$ ), as well as several combinational structures based on these [7].

Figure 1(a) illustrates the physical structure of the off-valve unit cell, while Fig. 1(b) shows it in various states between fully open and fully closed. In the valve, a high Laplace pressure meniscus in a trigger channel is used to inflate an occluding bubble into a main channel with a lower Laplace pressure meniscus. As the occluding bubble inflates, it narrows the cross-section of the main channel in that area and restricts fluid flow. Once the bubble completely occludes the channel, further fluid flow in it is near completely restricted. This concept has been used to successfully demonstrate a range of practical microfluidic operations, and proof-of-concept viscometry assay [8].

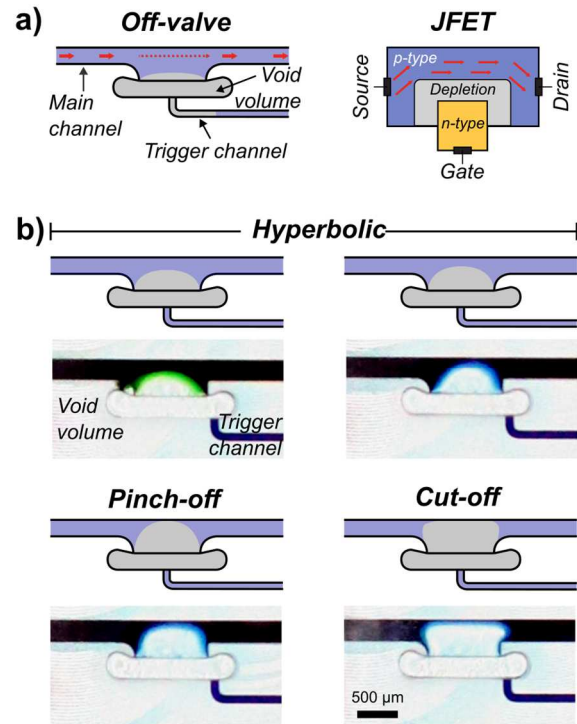


Figure 1: (a) Schematic comparing the capillary off-valve structure with a Junction Field Effect Transistor (JFET). The trigger channel length/volume provides input to an occluding air bubble, similar to the gate and depletion region in a JFET. (b) Schematics and optical micrographs of off-valves illustrating various occlusion states and their corresponding equivalents in a transistor model. Dye colored water was used to visualize flow through valves.

As is common in microfluidics, and capillarc circuits in particular, an electronic analogue exists for the capillary action off-valve. In the off-valve, the mechanism of an occluding bubble restricting fluid flow is like that of a depletion region in the junction field effect transistor (JFET). In both cases, a volume of non-conductive medium is introduced into a channel and restricts the flow of that medium inside it. Up to now, the capillary off-valve device has been operated in purely binary modes, including manipulating the structure of the trigger channel to evaluate basic logical functions [9]. In all these binary operations the volume of the trigger channel, or trigger channel network, was fabricated such that the occluding bubble always completely blocked the main channel and restricted fluid flow.

While binary modes constitute an important application for electronic JFET devices, a wide range of other non-binary applications exist, including

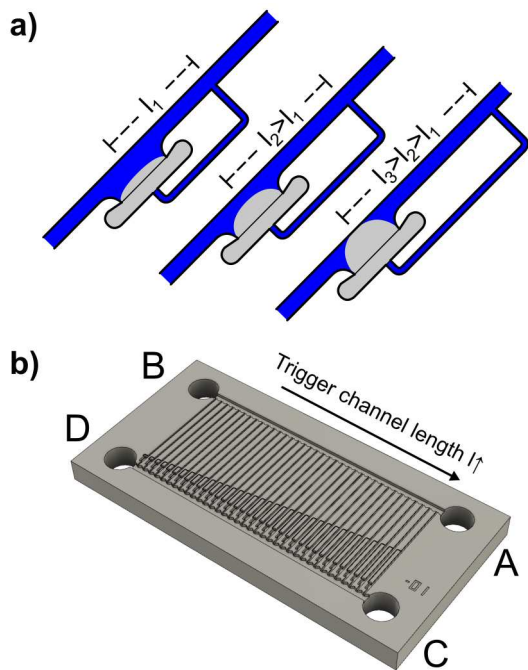


Figure 2: (a) Schematic illustrating the effect of trigger channel length, and thus volume, on air bubble size. Longer trigger channels lead to larger bubbles, allowing a range of states to be hard-coded. (b) Render of the PMMA test chip used to characterize flow behavior as function of trigger channel length. A total of 36 off-valves with differing trigger channel lengths were realized, covering states from fully open to cut-off. Labels A – D denote the position of inlets.

amplification, sensing, constant current sourcing and resistance modulation. All these applications would make impactful additions to the microfluidic toolkit. As such, inspired by well-established electronic applications and theoretical framework, this work provides a first investigation into the potential for analog operation of off-valves. In the following we demonstrate that the occluding bubble can be placed into a range of states between fully open and fully closed by modulating the trigger channel volume. Secondly, we apply a driving pressure and show that these bubble states correspond to a distinct range of flow resistances. Finally, we fit an existing transistor model (Shockley Equation) and use this to define transistor-like properties of the off-valve such as pinch-off volume.

## EXPERIMENTAL

To test the analog behaviour of the capillary off-valve structure, a test device was fabricated which placed 36 off-valve devices in parallel between two large fluid distribution channels. Figure 2(a) shows the method used to control the occluding bubbles volume. Along the width of the device the length of each trigger channel was adjusted while the depth was kept constant. This controlled the volume of each occluding bubble, and therefore the extent that it occluded the main channel of each off-valve. Figure 2(b) shows a CAD rendering of the test chip, illustrating arrangement of parallel off-valve testing channels, distribution channels and their inlets.

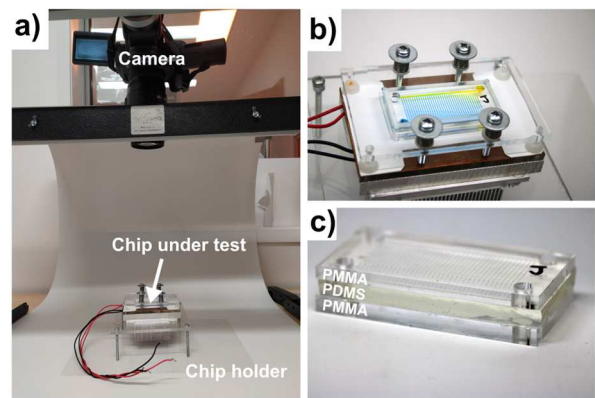


Figure 3: (a) Photograph of the experimental setup including the camera used to record fluid flow and the custom chip holder. Note that, while the chip holder incorporates temperature control, this was not used in the current work. (b) Close-up of the chip holder showing the frame used to clamp the device stack. (c) Photograph of a device stack consisting of the micro-milled PMMA chip and a PDMS cover forming a sandwich with a second flat piece of PMMA.

All flow experiments were conducted by addition of aqueous dye solutions (Brilliant Blue dye, #80717, Sigma Aldrich and Tartrazine, #T0388, Sigma Aldrich) into the reservoirs using a manual pipette. Liquid movement was recorded using a digital camera (Canon EOS 760D using a Canon Macro lens EF 100 mm 1:2.8 USM, recorded at 25 FPS). For testing, devices were initially filled from the C inlet using blue dye (Brilliant Blue). This filled each parallel branch of the device up to the point where parallel channels met the outlet distribution channel. At this point, flow into the outlet distribution channel was prevented by stop valve like structure which were formed by the sudden depth increase between the channels. Due to the self-triggering arrangement of the off-valves, where the trigger channel is automatically actuated upon filling of the device, each off-valve automatically actuated to its predetermined bubble volume.

To test the fluid resistance created by the occluding bubbles, all excess dye was removed from the D & C filling inlets using a manual pipette. The testing reservoir B was then filled using yellow dye (Tartrazine, #T0388, Sigma Aldrich). Hydrostatic pressure created by the filled inlet drove fluid flow through each channel, creating a change in colour due to the different dye colors. The uptake of these liquids was filmed, and could subsequently be used to track fluid flow via ImageJ [10], and Python 3 [11].

## Fabrication

Test devices used in this work were fabricated from cross-linked polymethylmethacrylate (PMMA; 4.5 mm general purpose acrylic; PSP Plastics) as previously described [8,9]. Channel milling was performed using a Mini-Mill/GX micro milling machine running a NSK-3000 Spindle (Minitech Machinery Corporation), with a minimum addressable step size of 1  $\mu\text{m}$ . Machining tools were purchased from Performance Micro Tool in diameters of 3.175 mm (SR-4-1250-S), 250  $\mu\text{m}$  (250M2X750S) and 100  $\mu\text{m}$  (100M2X300S) for the square heads and 200  $\mu\text{m}$

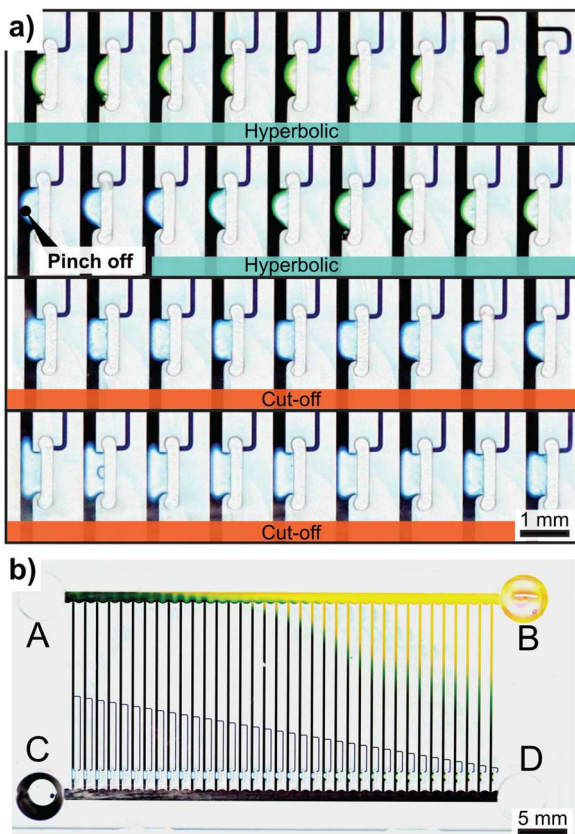


Figure 4: (a) Demonstration of the obtained range of bubble states. Using this approach the bubble volume, which pinches off the channel, can be identified. Regions before and after pinch off are labeled hyperbolic and cut-off regions, following the JFET conventions. (b) Photograph of the chip after completion of an experiment. Due to the varying size of each occluding bubble, fluid resistance of each channel was different. As a result, yellow dye flowed a different distance through each of the parallel channels. This allowed the fluid flow rate to be optically tracked.

(TR-2-0080-BN) for ball nose. Design files and milling parameters (G-code) were prepared CAD software (Autodesk Fusion 360<sup>®</sup> 2020 Autodesk, Version 2.0.10356) for all functional units.

Each sample was fabricated by an initial face cut (3.175 mm cutter) to level out the surface, followed by milling of each channel. The surface was then polished using acrylic polish (aluminium oxide-based CRC, code 9230), followed by ultra-sonication for 1 min in ~5% (v/v) aqueous isopropyl alcohol solution, washing with acetone, isopropyl alcohol and water and blow drying with nitrogen. To close microscopic cracks that arose during the milling process, the surface was coated with high molecular weight PMMA solution (average  $M_w = 996,000$ , 2.5% in xylene; Sigma Aldrich). Any remaining solvent was removed by drying samples at 90°C for 5 min on a hotplate and keeping the hot sample under vacuum for at least 1 min. Finally, samples were plasma-treated ten times for 1 min, each time at 25 W, pulsed mode (ratio 50) using O<sub>2</sub> gas (3 sccm; Tergeo Plasma Cleaner, Pie Scientific). A thin (2–3 mm) polydimethylsiloxane slab was prepared (PDMS; Sylgard

184, Electropar), mixed at 10:1 w:w base:curing agent and cured at 80°C for 2 h. This PDMS slab acted as hydrophobic cover for the chip and a frame holder ensured a tight seal of this to the PMMA channels. The camera setup, holder and chip stack are shown in Fig. 3(a-c).

## RESULTS

Figure 4(a) shows all the bubble states obtained using the test device. These states were reliable and repeatable across experiments on the same test device. The pinch-off volume in Fig. 4(a) is defined as the trigger channel volume which creates a bubble that only just occludes the main channel. This follows the convention of pinch-off voltage in an electronic JFET. In the channel geometry studied in this work, the pinch off volume,  $V_p$ , was determined to be 25.7 nL. While this value is specific to this particular off-valve geometry, it will also change with the compressibility of the gas used in the trigger channel.

Figure 4(b) shows a photograph of an overall result of a flow resistance test. In this experiment, the driving pressure is the hydrostatic pressure created by liquid at the testing inlet A. However, as liquid drains out of the devices, it re-fills the “filling” inlet C. This creates a capillary back pressure which opposes the applied hydrostatic pressure, meaning that the driving pressure is reduced as the experiment proceeds. After approximately 15 seconds, the capillary back pressure and the forward hydrostatic pressure reached equilibrium, and the experiment concludes. This effect allows Fig. 4(b) to conveniently represent the integrated fluid flow (equivalently, hydraulic resistance) through the parallel branches as a kind of bar graph. In this the hydraulic resistance of each capillary off-valve is modulated by the volume of its occluding bubble and the visually identified pinch-off volumes correspond closely with that demonstrated by Fig. 4(b).

When the fluid flow, which results in Fig. 4(b), is optically tracked, it can be quantified. This approach leads to the data shown in Fig. 5(a), which demonstrates how the capillary slows the fluid flow over time. To circumvent this aspect of the experimental design, a linear line was fitted to the beginning of the response (approximately the first 5 seconds), meaning each capillary off-valves fluid flow was measured at comparable driving pressures only. Figure 5(b) shows this normalised flow rate against the trigger channel volume, for multiple testing directions, which can be used to examine any potential effect the distribution channel might have. To this data, a modified Shockley transistor equation could be fitted in the form of

$$Q_D = Q_{SS} \left(1 - \frac{V_{tr}}{V_p}\right) \quad (1)$$

Where  $Q_D$  is the flow rate in the main channel,  $Q_{SS}$  the saturation flow rate,  $V_p$  the pinch off volume and  $V_{tr}$  the trigger channel volume. A best fit for this model was obtained for a pinch off volume of 26.7 nL. This closely aligns with the values obtained by visually inspecting the bubble states.

It should be noted that as Fig. 5(b) shows the normalised flow rate, this only demonstrates the consistency of the off-valves resistance control. The absolute variability of flow rate on the other hand was much larger, as driving pressure was uncontrolled between experiments. This leaves room for improvements in future

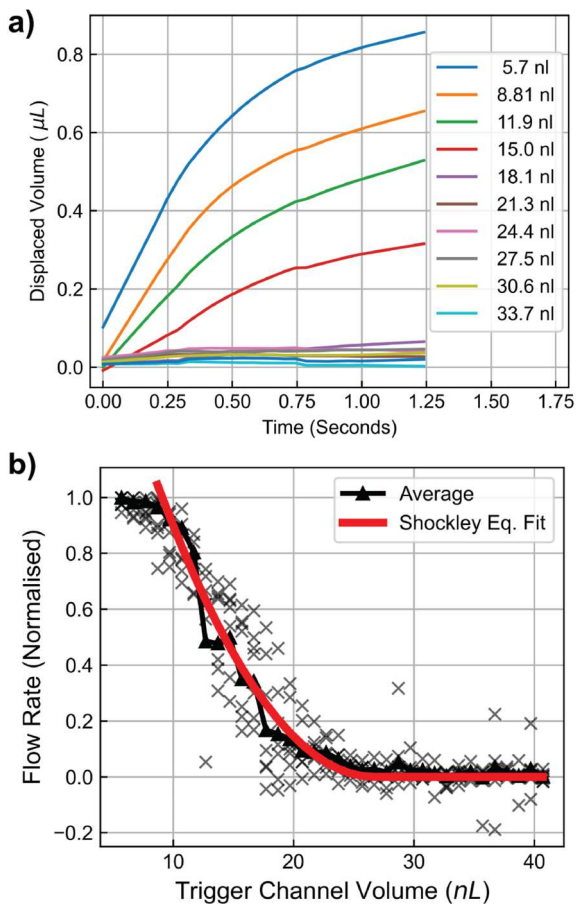


Figure 5: (a) Optically tracked fluid flow through a subset of the parallel off-valve branches. Flow in each branch begins quickly and slows as capillary back pressure in the outlet builds. (b) By fitting a linear regression to the beginning of the flow response, flow that each off-valve allows at a single pressure can be measured. When this response is plotted against trigger channel volume, a flow rate versus trigger channel volume curve can be established, which can be fitted with a modified Shockley transistor model.

work, which will characterize the transistor-like behaviour of the off-valves in greater detail.

## CONCLUSION

In this work we have demonstrated that capillary action off-valves can be controlled into analog states and as hydraulic resistances. So far testing pressures used have been small compared to the Laplace pressure of the occluding bubble. As a result, bubbles did not distort considerably under the influence of fluid flow. Thus, in this pressure range, the controllable resistance that the capillary off-valve represents can be considered a linear resistive device. This may not be the case for all driving pressure ranges, and in the future more work is needed to better understand this regime. The flow experiments also demonstrated that, to effectively control flow rate, driving pressure will need to be tightly controlled. In the future, we aim to increase the resistance of the capillary off-valve devices so that more dominant control of flow behaviour in capillary circuit devices can be achieved. This will be

made possible by reducing the cross-sectional area of the main channel, thus enabling devices based on off-valves to be used for PoC applications.

## ACKNOWLEDGEMENTS

The authors would like to thank Helen Devereux and Gary Turner of the University of Canterbury Nanofabrication Laboratory for technical support. Funding was provided by MBIE Grant UOCX1706. C.M. acknowledges the Japan Society for the Promotion of Science and V.N. Rutherford Discovery Fellowship RDF-19-UOC-019 for additional funding.

## REFERENCES

- [1] P. A. Tideman et al., "Impact of a regionalised clinical cardiac support network on mortality among rural patients with myocardial infarction," *Med. J. Aust.*, vol. 200, no. 3, pp. 157–160, 2014.
- [2] O. A. Soremekun, E. M. Datner, S. Banh, L. B. Becker, J. M. Pines, "Utility of point-of-care testing in ED triage," *Am. J. Emerg. Med.*, vol. 31, no. 2, pp. 291–296, 2013.
- [3] E. Lee-Lewandrowski and K. Lewandrowski, "Perspectives on Cost and Outcomes for Point-of-Care Testing," *Clin. Lab. Med.*, vol. 29, no. 3, pp. 479–489, 2009.
- [4] M. I. Mohammed, S. Haswell, I. Gibson, "Lab-on-a-chip or Chip-in-a-lab: Challenges of Commercialization Lost in Translation," *Procedia Technol.*, vol. 20, pp. 54–59, 2015.
- [5] C. Florkowski, A. Don-Wauchope, N. Gimenez, K. Rodriguez-Capote, J. Wils, A. Zemlin, "Point-of-care testing (POCT) and evidence-based laboratory medicine (EBLM) – does it leverage any advantage in clinical decision making?," *Crit. Rev. Clin. Lab. Sci.*, vol. 54, no. 7–8, pp. 471–494, 2017.
- [6] ISO/TC 212, "ISO 22870:2016," *ISO 22870:2016*, 2016. (accessed Aug. 12, 2021).
- [7] J. Menges, C. Meffan, F. Dolamore, C. Fee, R. Dobson, and V. Nock, "New flow control systems in capillaries: off-valves," *Lab Chip*, vol. 21, no. 1, pp. 205–214, 2021.
- [8] C. Meffan, J. Menges, F. Dolamore, D. Mak, C. Fee, V. Nock, R. Dobson, "A versatile capillary microfluidics viscometer platform for bar-graph type point-of-care diagnostics," *ChemRxiv*, 2021 <https://doi.org/10.33774/chemrxiv-2021-w0zc9>
- [9] C. Meffan, J. Menges, F. Dolamore, C. Fee, R. Dobson, V. Nock, "Transistor off-Valve Based Feedback, Metering and Logic Operations in Capillary Microfluidics," in *Proc. of IEEE MEMS'21 Conference*, Virtual, Jan. 2021, pp. 218–221.
- [10] J. Schindelin et al., "Fiji: an open-source platform for biological-image analysis," *Nat. Meth.*, vol. 9, no. 7, pp. 676–682, 2012.
- [11] G. Van Rossum and F. Drake, "Python 3 Reference Manual CreateSpace," *Scotts Val. CA*, 2009.

## CONTACT

\*V. Nock; tel: +64 3 3694303;  
volker.nock@canterbury.ac.nz